

Instantaneous, Zero-Feedback Fading Mitigation with Simple Backscatter Radio Tags

Georgios Vougioukas, Aggelos Bletsas, *Senior Member, IEEE* and
John N. Sahalos, *Life Fellow, IEEE*

Abstract—This work offers a novel, backscatter radio-based, blind beamforming technique that assists the reception of signals in multipath conditions. The technique is based on simple, assistive backscattering tags, implemented without any means of signal amplification. These tags can *blindly* (i.e., without feedback) modify the phase of the associated wireless channels, leading to constructive addition of the multipath components (i.e., alignment). Such alignment events offer distributed beamforming gain. Analysis is performed and an expression for the probability of alignment is offered, along with an expression for the achievable gain, corroborated by simulations and experimental results. It is shown that increased number of assistive tags offers higher beamforming gain, at the expense of increased delay. The effectiveness of the proposed beamforming technique is highlighted with experiments and measurements on the radio frequency identification (RFID) Gen2 standard. Commercial RFIDs that initially could not be interrogated due to insufficient impinging power, were successfully interrogated hundreds of times/minute with the assistance of the beamforming tags. It was experimentally shown that the proposed beamforming tags can offer power gains in the range of 0.4 – 3.7 dB. While the technique was tested on commercial RFIDs, it is not limited to a specific communication standard.

Index Terms—Beamforming, Backscatter Radio, RFID, Wirelessly Powered Communications.

I. INTRODUCTION

Beamforming has been traditionally employed in wireless communications for the purpose of increasing the signal power at an intended receiver. In the case of transmit beamforming, the transmitter is equipped with an antenna array. A common signal feeds the elements of the array and at each element, a different phase shift is introduced; by carefully controlling each of the aforementioned phases (and/or amplitude), certain areas in space can enjoy higher power levels compared to others. This is due to constructive and destructive addition of the signals emitted from each of the elements, in conjunction with the effect of the propagation environment. In receive

beamforming, the receiver is equipped with an array and the same operation is performed; each element of the receiver’s array “weights” the impinging signal with a different phase (and/or amplitude).

In a typical scenario of transmit beamforming, the transmitter is aware of the propagation environment and channel state information (CSI) is available to the transmitter using feedback from the receiver; the transmitter is able to adjust the weights at each element of the array (phase and/or amplitude), so that a specific metric at the receiver is maximized (e.g., SNR), under various constraints (e.g., transmit power) [1]. It is evident that given the need for an antenna array, i.e., multiple radio frequency (RF) front-ends, both the implementation complexity and the cost are critical issues in the realization of beamforming systems.

One solution to the complexity and cost of multiple RF front ends is based on parasitic arrays, such as switched parasitic antennas (SPAs) and electronically steerable passive array radiators (ESPARs) [2]. In such systems, a number of parasitic elements terminated with variable loads, are placed near a single active element. To ensure sufficient coupling, the parasitic elements are placed at distances of less than $\lambda/2$ from the active element. By altering the loads of the parasitics for a given stimulation of the single active element, different radiation patterns can be realized. Using such antenna systems, beamforming [3], MIMO communication [4], [5] and other problems requiring statistical signal processing [6], can be solved without multiple RF front ends. An SPA for a RFID reader was designed in [7]. The circuitry of the parasitic element was wirelessly powered from the driven element, altering the parasitic load periodically.

For some applications (e.g., sensor networks), multiple dislocated, synchronized, single antenna transmitters can cooperate, in order to achieve distributed beamforming. In that case, a signal that must be received at a specific location is *simultaneously* broadcasted by each of the distinct transmitters; each of the transmitters introduces a phase shift at the common signal and an overall beamforming gain is achieved towards the receiver [7]. In the case of distributed beamforming, the complexity of a conventional array (i.e., an array consisting of multiple RF front ends), is traded for the complexity of synchronizing multiple transmitters. Non-synchronized transmitters can be also employed, for *blind*, i.e., zero-feedback, distributed beamforming, as it was shown in [8]. In [9], a number of cooperative RFIDs was used to transmit the same signal towards a reader, thus offering diversity gain. Provided that the RFIDs were not forward link

G. Vougioukas’ research has been financially supported by General Secretariat for Research and Technology (GSRT) and the Hellenic Foundation for Research and Innovation (HFRI) (Scholarship Code: 2263). A. Bletsas’ and John N. Sahalos’ research has been co-financed by the European Union and Greek national funds through the Operational Program Competitiveness, Entrepreneurship and Innovation, under the call RESEARCH - CREATE - INNOVATE (project code: T1EDK-03032). Georgios Vougioukas and Aggelos Bletsas are with School of ECE, Technical Univ. of Crete, Kounoupidiana Campus, Chania, Crete, Greece 73100. tel. +30-28210-3737. John N. Sahalos is with Radio-Communications Laboratory (RCLab), Department of Physics, Aristotle University of Thessaloniki, Thessaloniki, Greece 54124, tel. +30-2310-998161 and Department of Engineering, University of Nicosia, Cyprus, email: gevougioukas@isc.tuc.cy.ac.cy, aggelos@telecom.tuc.cy.ac.cy, sahalos@auth.gr

limited, coarse synchronization was achieved by the reader initializing the readout, while symbol synchronization was facilitated by employing groups of tags offering little variation in their symbol timing.

There has been a lot of interest recently towards beamforming using distinct devices in the environment, rather than the transmitter or the receiver units; that is the case of re-configurable intelligent surfaces (RIS) [10]–[13]; the latter are surfaces that their electromagnetic behavior can be controlled electronically. Thus, the propagation environment can be altered and beamforming can be realized. Such surfaces may be implemented, among other ways, using reconfigurable reflectarrays [14] and programmable meta-surfaces [15]. In [16], an algorithm was designed for maximizing the received signal strength at target areas, by placing highly reflective metallic surfaces in specific spots.

In [17], a large array of dual-antenna elements, connected through phase shifters, was considered. Propagation was altered by controlling the phase shifters, i.e., a phase shift was applied to each signal received by the first antenna of each element and then re-transmitted by the second. Using channel feedback from a Wi-Fi access point, the phase shifters of the array were controlled in a way that specific performance goals could be achieved at a receiver (e.g., Shannon capacity). In [18], an array of column-wise connected (through RF switches) metallic patches altered the reflective area of a large surface. Depending on the state of each switch, the reflective area of the surface (and by extension the propagation environment) could be controlled. Exploiting received signal strength indication (RSSI) feedback from the receiver, a controller could assign appropriate states at each switch so that power at the receiver's location could be maximized.

Binary reconfigurable, large metasurfaces, able to enhance the reception of RF signals on a communication system are also proposed in [19]. The control of the said metasurfaces is performed through custom optimization algorithms, utilizing channel feedback from a secondary¹ receiver connected to the controller; a transmitter of the said communication system may also be connected (through network infrastructure) to the controller of the surface [20]. A similar technique was presented in [21].

Shifting the functionality required for beamforming from the radio ends to the environment may suggest large surfaces/RIS, requiring additional installation effort, as well as custom controllers with elaborate algorithms. The last, require channel feedback so as to appropriately control the surface; cooperation with the legacy communication system, i.e., the system to be assisted by the beamforming operation, or in some cases with an additional, secondary, receiver is required for the said feedback, which may not be an option for many practical scenarios.

This work offers simple, assistive, backscatter radio tags that can assist the reception of signals subject to harsh propagation conditions [22]. A backscattering [23], assistive tag, capable of reflecting an impinged signal (with altered phase) is designed and implemented. By varying the antenna

load of the assistive tag using a varactor (or discrete loads), the phase introduced to the reflected/backscattered signal can be varied continuously, throughout a wide range of values. The last, effectively modifies the propagation environment by introducing “controllable” multipath propagation components; depending on the phase introduced by the assistive tag, areas in space will enjoy constructive (or destructive) addition of the multipath signal components. Thus, a receiver placed in a fixed location will be favored, if the phase introduced by the assistive tag leads to a constructive addition of signals at the said location.

It must be emphasized that the proposed assistive tag does not need to (actively) amplify the signal. The proposed instantaneous beamforming system was tested on the RFID Gen2 standard, assisting the interrogation of RFID tags that could not (otherwise) be “activated”, due to insufficient impinged power (due to multipath). The passive nature of the beamforming tags showcases the feasibility of a setup where adjacent, beamforming-capable RFID tags can help each other. For example, in a large storage facility where multiple RFIDs are deployed (in the stored items) and the interrogation system is permanently installed, there could exist spots where the power is below the sensitivity threshold of a RFID (at that spot). Adjacent RFIDs, equipped with the proposed instantaneous beamforming capability can help the troubled RFID so as to be successfully interrogated.

While this work utilizes the RFID Gen2 communication standard, the principle is not limited to a specific protocol; any receiver, subject to harsh multipath conditions, can be aided by the utilization of properly designed assistive tags (provided that the instantaneous nature of the suggested beamforming method is beneficial to the said receiver). Extensive experimental channel measurements, verify the applicability and effectiveness of the proposed technique.

Contrary to RIS-related prior art, the proposed low-complexity assistive tags, do not rely on receiver feedback; control of the assistive tags' varactor/load (and by extension the assistive tag's phase) is *blind*. The blind/zero-feedback control is based on continuously varying the phase introduced by the assistive tag, in a predefined pattern. That pattern depends on the radio standard to be aided by the assistive tags. By blindly controlling the phase throughout a wide range of values and given an area in space, there will be points in time that the multipath components will add constructively. The extent of areas enjoying (maximum) gain due to constructive addition events, will depend on the assistive tag's design (value range of the backscattering phase & scattering characteristics) and the propagation conditions.

Based on the framework developed in [8], an expression offering the probability of constructive addition events (subsequently referred to as alignment events) will be offered and verified through simulations. An analytical expression for the achievable gain will be also offered and verified through both simulations and experimental channel measurements. Given non-favorable multipath conditions and a certain phase introduced by the assistive tag, destructive addition may also take place. As will be later discussed, depending on the application, this phenomenon may not be a serious drawback of the system.

¹Primary being the receiver of the said communication system.

In summary, this work offers the following contributions:

- In contrast to deploying large RISs, associated with feedback structures & control algorithms, this work offers a simple, *zero-feedback*, backscatter radio-based, fading mitigation/beamforming technique & prototype, for coping with the effects of multipath.
- Due to the blind/zero-feedback nature of the proposed beamforming system, analysis is performed and an expression is offered for the probability of alignment. The derived expression is verified through simulations.
- An analytical expression for the average power gain offered by a (given) number of assistive (beamforming) backscattering tags, is derived, verified through simulations and corroborated by experimental results.
- Despite the passive nature of the proposed beamforming tags, extensive measurements showed that considerable gains (in the order of 3 dB) can be enjoyed, even when utilizing a single tag.
- The feasibility and effectiveness of the proposed beamforming technique, is highlighted with experiments and measurements utilizing the commercial Gen2 protocol; RFID tags were successfully interrogated multiple times only after the aid of the proposed, assistive, backscattering tags.
- The simple, passive (no amplification) character of the beamforming tag(s), allows for future, wirelessly powered (beamforming) tags, to aid the interrogation of other, adjacent, RFID tags that could not otherwise operate due to the effects of multipath.

The rest of the work is organized as follows. The signal model is offered in Sec. II and the effect of the assistive tag on the received signal is shown. In Sec. III, expressions for the probability of alignment/constructive addition and the achievable power gain are derived, while in Sec. IV details regarding the design and implementation of the assistive tag are given. Simulation and experimental results are given in Sec. V and work is concluded in Sec. VI.

II. SIGNAL MODEL AND BASIC IDEA

Flat fading is assumed, with $h_d = a_0 e^{-j\phi_0}$ complex scale factor, $a_0 \in \mathbb{R}_+$, $\phi_0 \in [0, 2\pi)$, characterizing the effect of multipath between transmitter and receiver [24]. Assuming transmission amplitude $\sqrt{2P_{\text{tx}}}$ at center (carrier) frequency of F_c , the impinging signal at the receiver can be simplified to:

$$r_G(t) = \sqrt{2P_{\text{tx}}} \Re \left\{ h_d e^{j2\pi F_c t} \right\}, \quad (1)$$

where $\Re \{z\}$ denotes the real part of complex z . As a case study example, this work will use commercial Gen2 RFID to experimentally demonstrate the benefits of the proposed techniques. In that case, a RFID tag at location G receives the above signal, however the impinging power is not strong enough, and thus, tag's RF energy harvesting circuits fail to activate it; hence, the RFID tag cannot be read from the illuminating reader (depicted in Fig. 1-middle).

Assume now that an "assistive" tag is placed in the vicinity of the transmitter-receiver/RFID link. That tag adds another path between transmitter and receiver, denoted through the

complex coefficient h_1 , altering the impinging signal at the receiver, as follows:

$$r_G(t) = \sqrt{2P_{\text{tx}}} \Re \left\{ (h_d + h_1(t)) e^{j2\pi F_c t} \right\}, \quad (2)$$

where $h_d + h_1(t)$ expresses the overall multipath contribution in the link, introduced by the environment and the "assistive" tag. If the two complex coefficients h_d , h_1 or equivalently their representation vectors align towards the same direction, then there will be constructive addition that further enhances the impinging signal at the receiver. On the other hand, the phases of the equivalent channel vectors may offer destructive addition, further weakening the received signal. In this work, the "assistive" tag changes periodically the phase of h_1 , so that its vector representation rotates in the complex plane, ensuring time intervals with constructive alignment between h_d and h_1 (depicted in Fig. 1-right). It is emphasized that the rotation of h_1 due to assistive tag's operation is necessary, as the latter receives no feedback from the receiver, regarding the appropriate phase to be selected that offers constructive addition and hence, *beamforming gain*.

For the special case of RFID reception, the "assistive" tag boosts the power of the impinging signal at location G, where the tag there can now be sufficiently powered and thus, successfully interrogated (Fig. 1-right). Such effect will be experimentally demonstrated in Section V of this work.

The assistive tag can manifest such change of $h_1(t)$, using backscatter radio principles, even though it may be fixated at a specific location. Specifically, the assistive tag terminates its antenna to a variable load, which in turn modifies its reflection coefficient; the latter controls the phase of the signal reflected from the assistive tag, toward the receiver. More specifically, the aforementioned factor is expressed as:

$$h_1(t) = h_{\text{RA}}^{(1)} s_1 \left(A_s^{(1)} - \Gamma_1(t) \right) h_{\text{AG}}^{(1)}, \quad (3)$$

where $h_{\text{RA}}^{(1)}$, $h_{\text{AG}}^{(1)}$ are the complex parameters that represent the wireless channel from transmitter/reader to assistive tag and from assistive tag to receiver, respectively. Tag's scattering efficiency is expressed by $s_1 \in (0, 1)$, while $A_s^{(1)} \in \mathbb{C}$ denotes the structural mode of the tag's antenna, which in principle does not depend on the terminating load but only on the electrical and geometrical properties of the antenna [25]. The term $A_s^{(1)} - \Gamma_1$ controls the signal reflected from the assistive tag, while parameter s_1 models the scattering efficiency, which in practice may be non-ideal. The assistive tag can alter the loading of its antenna, attaining different reflection coefficients [26]:

$$\Gamma_1(t) = \frac{Z_1(t) - Z_a^*}{Z_1(t) + Z_a}, \quad \Gamma_1(t) \in \mathbb{C}, \quad (4)$$

where $Z_1(t)$ denotes the load terminating the tag's antenna at time instant t and Z_a the impedance of the same antenna. Clearly, varying the assistive tag's terminating load modifies the reflection coefficient, which in turn modifies the phase of h_1 . Simple, passive (i.e., without amplification) circuitry to implement such operation will be provided in Section IV. It is further noted that reflection may not be necessarily passive, i.e., the assistive tag may also utilize a reflection amplifier to

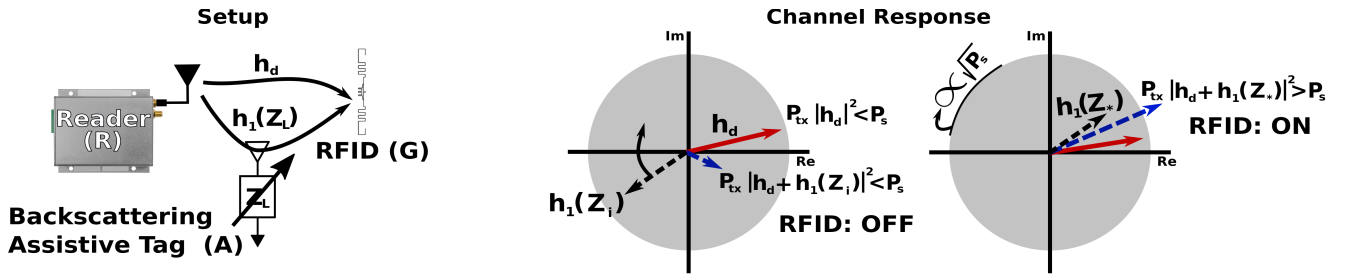


Fig. 1: The basic idea behind this work: a commodity wireless transmitter-receiver link is aided by the presence of backscattering assistive tag(s). The presence and operation of each assistive tag periodically alters the propagation environment, leading to constructive addition of the reflected paths at certain time intervals, offering a stronger channel and received signal at an intended receiver. RFIDs that could not be interrogated due to insufficient impinging power (below sensitivity threshold P_s), were successfully interrogated 100s of times/minute, with the aid of the proposed assistive tags.

reflect-and-amplify, simultaneously. In that case, parameter s or amplitude of Γ may assume values greater than 1.

More than one assistive tags may be utilized, which operate independently. In that scenario, the received signal at location G is given by:

$$\begin{aligned} r_G(t) &= \sqrt{2P_{tx}} \Re \left\{ \left(h_d + \sum_{m=1}^M h_m(t) \right) e^{j2\pi F_c t} \right\} \\ &= \sqrt{2P_{tx}} \Re \left\{ h(t) e^{j2\pi F_c t} \right\}, \end{aligned} \quad (5)$$

where M is the number of assistive tags; $h_m(t)$ follows Eqs. (3), (4), where index 1 is substituted by m .

III. ANALYSIS

A. Compound Wireless Channel

Denoting $h_{RA}^{(m)} \triangleq \sqrt{L_{RA}^{(m)}} a_{RA}^{(m)} e^{-j\phi_m}$, $a_{RA}^{(m)} \in \mathbb{R}_+$, $\phi_m \in [0, 2\pi)$ and $h_{AG}^{(m)} \triangleq \sqrt{L_{AG}^{(m)}} a_{AG}^{(m)} e^{-j\phi'_m}$, $a_{AG}^{(m)} \in \mathbb{R}_+$, $\phi'_m \in [0, 2\pi)$, the following holds:

$$\begin{aligned} h(t) &\triangleq h_d + \sum_{m=1}^M h_m(t) \\ &= \sqrt{L_0} a_0 e^{-j\phi_0} + \sum_{m=1}^M \tilde{\gamma}_m(t) e^{-j(\phi_m + \phi'_m - \Theta_m(t))}, \end{aligned} \quad (6)$$

where $\tilde{\gamma}_m(t) \triangleq \sqrt{L_{RA}^{(m)} L_{AG}^{(m)}} a_{RA}^{(m)} a_{AG}^{(m)} s_m \gamma_m(t)$, $\gamma_m(t) e^{j\Theta_m(t)} \triangleq (A_s^{(m)} - \Gamma_m(t))$, $\gamma_m(t) \in \mathbb{R}_+$, $\Theta_m(t) \in [0, 2\pi)$. The direct link pathloss is defined as $L_0 = G_R G_A \left(\frac{\lambda}{4\pi}\right)^2 \frac{1}{d_0^2}$, where d_0 the reader to RFID (G) distance. Parameters $L_{RA}^{(m)}$, $L_{AG}^{(m)}$ model the pathloss of the reader-to- m th assistive and m th assistive-to-RFID links, respectively:

$$L_{RA}^{(m)} = G_R G_A \left(\frac{\lambda}{4\pi}\right)^2 \frac{1}{d_{m,RA}^2}, \quad L_{AG}^{(m)} = G_A G_G \left(\frac{\lambda}{4\pi}\right)^2 \frac{1}{d_{m,AG}^2}, \quad (7)$$

where G_R , G_A , G_G the gains of the reader's, assistive tag's and RFID's antennas, respectively. $\lambda = \frac{3 \cdot 10^8}{F_c}$ denotes the wavelength and $d_{m,RA}$, $d_{m,AG}$ the reader-to- m th assistive and m th assistive-to-RFID distances, respectively.

Time is split in slots; in each slot k , a different load is connected to the antenna of the assistive tag. The duration of each slot, based on the transmitter-receiver link bit rate and packet length properties, accommodates $N_G \geq 1$ complete transmission phases, i.e., interrogations. Each transmission phase/interrogation describes one complete packet transmission, including all necessary handshaking between transmitter and receiver. It is further assumed that all wireless channel parameters are block-constant for each interrogation and vary randomly between successive interrogations. Tag circuit & antenna related parameters are assumed to be constant. Hence, wireless channel parameters have been modified between consecutive slots and Eq. (6) can be rewritten on a per-slot way, as follows:

$$h[k] = \sqrt{L_0} a_0 e^{-j\phi_0} + \sum_{m=1}^M \tilde{\gamma}_m[k] e^{-j(\phi_m + \phi'_m - \Theta_m[k])}. \quad (8)$$

The maximum beamforming gain is achieved when all of the two-dimensional vectors² involved in Eq. (8), align with each other. In other words, when all of these vectors align, maximum power is offered at location G of the receiver. Exact alignment is not necessary; beamforming gain can be enjoyed at location G, even when the individual vectors align within a specific sector. As it will be shown in Sec. III-E, a larger spread of the angles leads to a combined channel of smaller magnitude. By extension, allowing for a larger sector limits the maximum achievable beamforming gain.

Besides causing constructive addition at some slot k_c , the rotating vector (due to $\Theta_m[k]$), may result in destructive addition at some other slot k_d . Since the goal is to achieve successful reception at least once (e.g., at k_c), that drawback is not considered a serious issue. However, as will be shown in Sec. V-A, several slots may be needed until an alignment event and therefore, delay issues may arise.

B. Phase Alignment

As stated in the previous subsection, beamforming gain is offered when all the vectors (see Eq. (8)) add constructively

²Each complex channel coefficient is viewed as a phasor on the complex, two-dimensional plane, as shown in Fig. 1.

or, equivalently, the angles of these vectors align within a specified sector. The above can be informally stated as follows:

$$\begin{aligned} \phi_i + \phi'_i - \Theta_i[k] &\approx \phi_j + \phi'_j - \Theta_j[k], \\ \forall i, j &\in \{0, 1, \dots, M\}, \text{ with } i \neq j. \end{aligned} \quad (9)$$

The aforementioned constraint can be expressed formally as:

$$\begin{aligned} \cos\left(\phi_i + \phi'_i - \Theta_i[k] - \left(\phi_j + \phi'_j - \Theta_j[k]\right)\right) &\geq \cos(\epsilon), \\ \forall i, j &\in \{0, 1, \dots, M\}, \text{ with } i \neq j, \end{aligned} \quad (10)$$

where ϵ defines the alignment sector angle. It is also noted that notation-wise, $\phi_0 + \phi'_0 - \Theta_0[k] \equiv \phi_0$ ($\phi'_0 = \Theta_0[k] = 0, \forall k$) since index $m = 0$ is reserved for modelling the direct channel parameters (i.e., $h_d = \sqrt{L_0}a_0e^{-j\phi_0}$).

C. Probability of Alignment

It is assumed that the probability density function (PDF) of $\Phi_m \triangleq \phi_m + \phi'_m$, $f_{\Phi_m}(\Phi_m)$ is available. Additionally, phases $\Theta_m[k]$ are known.³ For the k -th slot,

$$\bar{\phi}_m^k = \Phi_m - \Theta_m[k]. \quad (11)$$

The probability density function (PDF) of $\bar{\phi}_m^k$ is given by $f_{\bar{\phi}_m^k}(\bar{\phi}_m^k) = f_{\Phi_m}(\bar{\phi}_m^k + \Theta_m[k])$ [27]. Accordingly, the cumulative distribution function (CDF) of $\bar{\phi}_m^k$ is given by $F_{\bar{\phi}_m^k}(x) = F_{\Phi_m}(x + \Theta_m[k])$. Next, $[0, 2\pi)$ -limited $\tilde{\phi}_m^k = (\bar{\phi}_m^k \bmod 2\pi)$ random variables (r.v.) are defined, with PDF(s) given by [28]:

$$\begin{aligned} f_{\tilde{\phi}_m^k}(\tilde{\phi}_m^k) &= \sum_{n \in \mathbb{Z}} f_{\bar{\phi}_m^k}(\tilde{\phi}_m^k + n \cdot 2\pi) \\ &= \sum_{n \in \mathbb{Z}} f_{\Phi_m}(\tilde{\phi}_m^k + n \cdot 2\pi + \Theta_m[k]). \end{aligned} \quad (12)$$

The CDF of (each) $\tilde{\phi}_m^k$ can be expressed as:

$$\begin{aligned} F_{\tilde{\phi}_m^k}(x) &= \int_0^x f_{\tilde{\phi}_m^k}(u) du \\ &= \int_0^x \sum_{n \in \mathbb{Z}} f_{\Phi_m}(u + n \cdot 2\pi + \Theta_m[k]) du \\ &\stackrel{(1)}{=} \sum_{n \in \mathbb{Z}} \int_{n \cdot 2\pi + \Theta_m[k]}^{x + n \cdot 2\pi + \Theta_m[k]} f_{\Phi_m}(\xi) d\xi \\ &= \sum_{n \in \mathbb{Z}} [F_{\Phi_m}(x + n \cdot 2\pi + \Theta_m[k]) \\ &\quad - F_{\Phi_m}(n \cdot 2\pi + \Theta_m[k])] \\ &= \sum_{n \in \mathbb{Z}} F_{\Phi_m}(x + n \cdot 2\pi + \Theta_m[k]) \\ &\quad - \underbrace{\sum_{n \in \mathbb{Z}} F_{\Phi_m}(n \cdot 2\pi + \Theta_m[k])}_{\text{Fixed given } n, \Theta_m[k]}, \quad x \in [0, 2\pi), \end{aligned} \quad (13)$$

³As it can be seen, the analysis is not limited to known assistive tag phases. Randomness can be introduced to $\Theta_m[k]$. In such case, the characteristics of $\Theta_m[k]$ must be taken into account in the calculation of relevant probability density function (PDF) and cumulative distribution function (CDF).

where in (1), the substitution $\xi = u + n \cdot 2\pi + \Theta_m[k]$ was performed. Using Eq. (10), the probability of alignment (at slot k) is defined as:

$$p[k] \triangleq \mathbb{P}\left(\bigcap_{i \neq j} \cos(\bar{\phi}_i^k - \bar{\phi}_j^k) \geq \cos(\epsilon)\right). \quad (14)$$

It can be shown [8], that for a collection of random variables $\{\bar{\phi}_m^k\}_{m=0}^M$, $p[k]$ can be lower-bounded, as follows:⁴

$$p[k] \geq \mathbb{P}\left(\max\{\bar{\phi}_m^k\}_{m=0}^M - \min\{\bar{\phi}_m^k\}_{m=0}^M \leq \epsilon\right). \quad (15)$$

Using results from [8], the lower bound of Eq. (15) will be calculated. Let $y = \min\{\bar{\phi}_m^k\}_{m=0}^M$ and $x = \max\{\bar{\phi}_m^k\}_{m=0}^M$. The joint PDF of the aforementioned variables is given by:

$$f(y, x) = \begin{cases} g(y, x), & y \leq x \\ 0, & \text{otherwise} \end{cases}, \quad (16)$$

where $g(y, x)$ is defined as [8]:

$$\begin{aligned} g(y, x) &= \sum_{(\beta_1, \beta_2), \beta_1 \neq \beta_2} \left[f_{\bar{\phi}_{\beta_1}^k}(y) f_{\bar{\phi}_{\beta_2}^k}(x) + f_{\bar{\phi}_{\beta_1}^k}(x) f_{\bar{\phi}_{\beta_2}^k}(y) \right] \times \\ &\quad \times \prod_{\beta_3, \beta_3 \neq \beta_1, \beta_3 \neq \beta_2} \left(F_{\bar{\phi}_{\beta_3}^k}(x) - F_{\bar{\phi}_{\beta_3}^k}(y) \right), \end{aligned} \quad (17)$$

and $\beta_1, \beta_2, \beta_3 \in \{0, 1, 2, \dots, M\}$. Finally, probability $p[k]$ can be bounded as:

$$\begin{aligned} p[k] &\geq \mathbb{P}\left(\max\{\bar{\phi}_m^k\}_{m=0}^M - \min\{\bar{\phi}_m^k\}_{m=0}^M \leq \epsilon\right) = \\ &= \int_{y=0}^{2\pi} \int_{x=y}^{\min\{y+\epsilon, 2\pi\}} f(y, x) dx dy. \end{aligned} \quad (18)$$

D. Average Number of Alignment Events

In this section, assuming N_s slots, the average number λ_a of alignment events per N_s slots will be calculated. First, the following binary random variable is defined:

$$\delta[k] = \begin{cases} 1, & p[k] \\ 0, & 1 - p[k]. \end{cases} \quad (19)$$

Using Eq. (19) the number of successful alignment events in N_s slots is given by the random variable $\delta_s = \sum_{k=1}^{N_s} \delta[k]$. Using Eq. (19), the average number of successful alignment events per N_s slots can be expressed as:

$$\lambda_a(N_s) = \mathbb{E}[\delta_s] = \sum_{k=1}^{N_s} \mathbb{E}[\delta[k]] = \sum_{k=1}^{N_s} p[k]. \quad (20)$$

E. Achievable Gain

Using Eq. (8) and given an alignment event, the reader-to-RFID channel attains the following form:

$$h^* = \sqrt{L_0}a_0e^{-j\phi_0} + \sum_{m=1}^M \tilde{\gamma}_m e^{-j\tilde{\phi}_m} = \sum_{m=0}^M \tilde{\gamma}_m e^{-j\tilde{\phi}_m}, \quad (21)$$

⁴For $\epsilon < \frac{\pi}{4}$ the lower bound is tight.

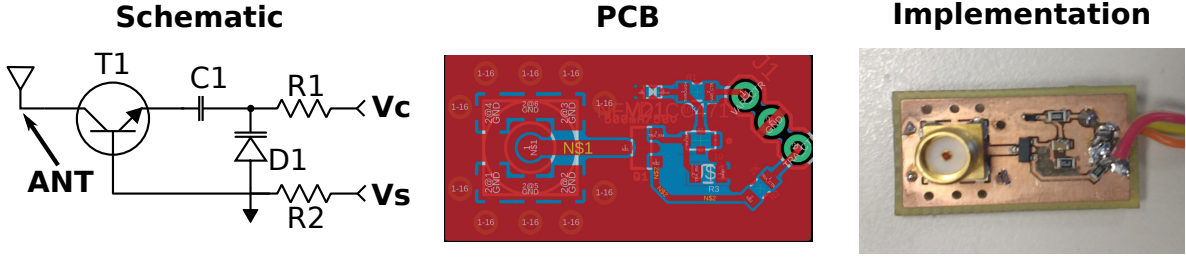


Fig. 2: Design and printed circuit board (PCB) implementation of the assistive tag. The values of R1 and R2 are 10 k Ω and 2 k Ω , respectively.

where $\tilde{\gamma}_0 e^{-j\bar{\phi}_0} = \sqrt{L_0} a_0 e^{-j\phi_0}$ denotes the direct link channel h_d . The (instantaneous) impinging power P_G at the RFID, can be expressed as (see Eq. (5)):

$$\begin{aligned}
 P_G &= P_{\text{tx}} |h^*|^2 = P_{\text{tx}} \left| \sum_{m=0}^M \tilde{\gamma}_m e^{-j\bar{\phi}_m} \right|^2 \\
 &= P_{\text{tx}} \left| \sum_{m=0}^M \tilde{\gamma}_m \cos(\bar{\phi}_m) - j \tilde{\gamma}_m \sin(\bar{\phi}_m) \right|^2 \\
 &= P_{\text{tx}} \left[\left(\sum_{m=0}^M \tilde{\gamma}_m \cos(\bar{\phi}_m) \right)^2 + \left(\sum_{m=0}^M \tilde{\gamma}_m \sin(\bar{\phi}_m) \right)^2 \right] \\
 &= P_{\text{tx}} \left[\sum_{m=0}^M \tilde{\gamma}_m^2 + 2 \sum_{m=0}^M \sum_{i=m+1}^M \tilde{\gamma}_m \tilde{\gamma}_i \cos(\bar{\phi}_m) \cos(\bar{\phi}_i) \right. \\
 &\quad \left. + 2 \sum_{m=0}^M \sum_{i=m+1}^M \tilde{\gamma}_m \tilde{\gamma}_i \sin(\bar{\phi}_m) \sin(\bar{\phi}_i) \right] \\
 &= P_{\text{tx}} \left[\sum_{m=0}^M \tilde{\gamma}_m^2 + 2 \sum_{m=0}^M \sum_{i=m+1}^M \tilde{\gamma}_m \tilde{\gamma}_i \cos(\bar{\phi}_m - \bar{\phi}_i) \right]. \quad (22)
 \end{aligned}$$

Assuming alignment within a sector of size ϵ , it holds that $\cos(\bar{\phi}_m - \bar{\phi}_i) \geq \cos(\epsilon) \forall m, i \in \{0 \dots M\}$. Thus, P_G can be lower-bounded as follows:

$$P_G \geq P_{\text{tx}} \left[\sum_{m=0}^M \tilde{\gamma}_m^2 + 2 \sum_{m=0}^M \sum_{i=m+1}^M \tilde{\gamma}_m \tilde{\gamma}_i \cos(\epsilon) \right] = \tilde{P}_G. \quad (23)$$

The (instantaneous) gain can be then approximated as $\tilde{G}_B = \frac{\tilde{P}_G}{P_{\text{tx}} L_0 a_0^2}$. If expected values are used instead of instantaneous, the average gain can be expressed as:

$$\mathbb{E}[\tilde{G}_B] = \frac{\sum_{m=0}^M \mathbb{E}[\tilde{\gamma}_m^2] + 2 \sum_{m=0}^M \sum_{i=m+1}^M \mathbb{E}[\tilde{\gamma}_m] \mathbb{E}[\tilde{\gamma}_i] \cos(\epsilon)}{L_0 \mathbb{E}[a_0^2]}. \quad (24)$$

It can be seen that if a certain gain is to be satisfied (e.g., to overcome RFID's sensitivity threshold), alignment within a narrower sector (smaller ϵ) may be required.

It is noted that if full description of the propagation environment and knowledge of the RFIDs' locations was available, appropriate placement and loading of the assistive tags could be performed. However, acquiring such information is not straightforward and feedback to the assistive tags is also mandatory, defeating the purpose of this work.

IV. IMPLEMENTATION

A. Tag Design

A backscattering tag was designed to implement the functionality described in Sec. II. The tag was able to alter the termination load of its antenna throughout a wide range of values (Fig. 2). The design is similar to the tag used in [29] for measuring the antenna's structural mode. A varactor was chosen to implement such task. The varactor of choice was an NXP BB179 (D1). An SMA connector was used to connect the antenna (Ettus VERT900) to an Avago AT-32033 BJT (T1) transistor and the emitter of the BJT was coupled to the varactor's cathode through a Murrata 470 pF (or 220 pF for tag #2) feed through capacitor (C1, see Fig. 2).

Besides enabling activation and deactivation of the assistive tag, transistor T1 "biases" the impedance range of the varactor towards a wider range of values. Different transistors were tested (e.g., NXP BFU20XRR); however, the chosen above offered the widest range of impedance values (as shown in Fig. 3). Based on the [aforementioned design choices](#), a printed circuit board (PCB) was designed and fabricated in-house, shown in Fig. 2.

B. Phase Control

The varactor has the ability to alter its capacitance as a function of the applied voltage. The diode has to be reverse biased in order to (properly) function as a voltage-controlled variable capacitor. A waveform generator was used to drive the cathode of the diode via resistor R1 (voltage/signal V_c , see Fig. 3). A linear upramp waveform was chosen for V_c at a frequency of 10 Hz. The voltage output swing of the generator was limited to 20 V_{pp}. Thus, the varactor's potential could not be fully exploited; BB179's cathode can be driven up to the maximum value of 30 V. To evaluate the offered range, the tag was connected to the generator and the impedance was measured using a VNA. The VNA was configured to CW mode (867.5 MHz) with an output power of -10 dBm. The impedance range for a full cycle of the upramp is shown in the Smith chart of Fig. 3. The inductive behavior is due to the presence of the BJT. The phase of the assistive tag's reflection coefficient is also offered in the same figure, along with the channel response resulting from the operation of the assistive tag (details are given in Sec. V).

The reflection coefficient phases of two different assistive tags, implemented with different coupling capacitors (C1) for

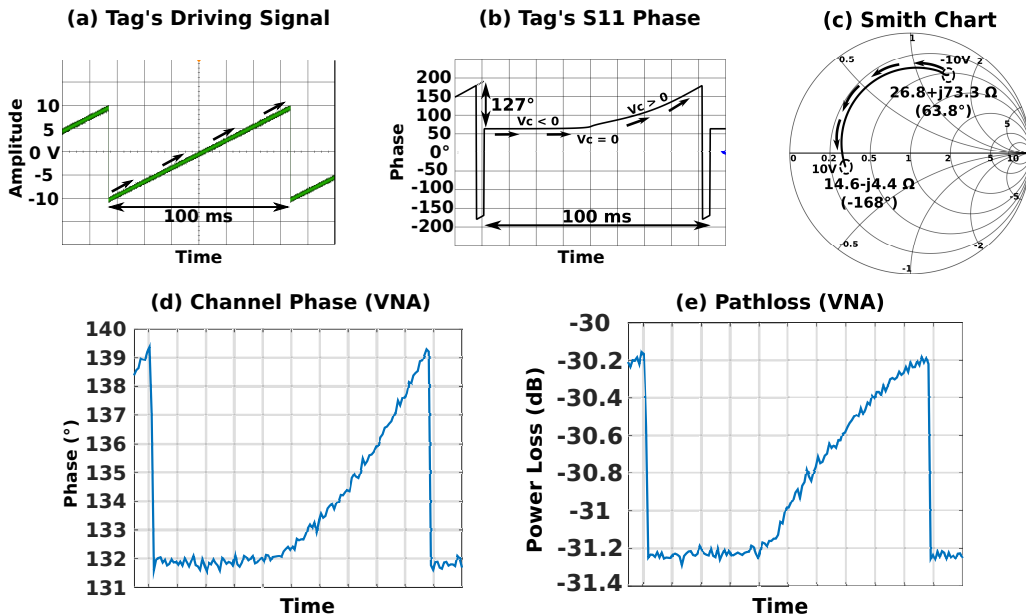


Fig. 3: Tag is driven by the signal shown in the oscilloscope capture (a). Phase of the reflection coefficient is shown in (b) and the impedance range in the Smith Chart in (c). The phase of the reflection coefficient, does not include the phase of the tag's structural mode term ($A_s^{(m)}$). The phase of the channel ($h_d + h_1(t)$) response as measured by a two-port vector network analyser (VNA, see Sec. V-C), is shown in (d); even though the variation of aggregate phase is limited, the resulting gain depends on the alignment of the individual channel components and the channel's aggregate phase is irrelevant (see Eq. (22)). The pathloss of the channel is also given in (e). It has to be noted that the pathloss without the tag present was -33.8 dB.

various voltage values applied to R1, are given in Fig. 4. It must be noted that, while most of the capacitance range is offered with the diode reverse biased, a limited range of phase/impedance values was offered by forward biasing the diode up to 10 V (lower saturation region in Fig. 4); the forward current was monitored to prevent diode's damage.

While the (utilized) diode requires relatively high voltages to achieve its full capacitance (and by extension phase) range, due to its reverse bias operation it draws (ideally) no current. Thus, given a properly designed, ultra-low-power voltage boosting circuit, batteryless/wireless powered operation is feasible. Besides, as it will be shown in Sec. V-C2, beamforming gain is also offered for binary loading (switching between two appropriate loads/diode voltages) of the assistive tag's antenna.⁵ The last showcases the feasibility for future RFIDs to be equipped with the appropriate circuitry that allows for instantaneous beamforming towards adjacent RFIDs.

1) *Period of Control Voltage Signal*: As stated in Sec. III-A, the phase introduced by the assistive tag(s) in a given slot affects multiple interrogations, while the wireless channel parameters remain block-constant for each interrogation and vary (randomly) between successive interrogations. Thus, the minimum time duration of a slot must be equal to the duration of a single transmission/interrogation ($N_G \geq 1$). In a different case, the operation of the assistive tag may interfere with the reception at the reader: the assistive tag will vary the channel's phase too "fast", effectively creating a non-block-constant wireless channel. As stated earlier, the duration of

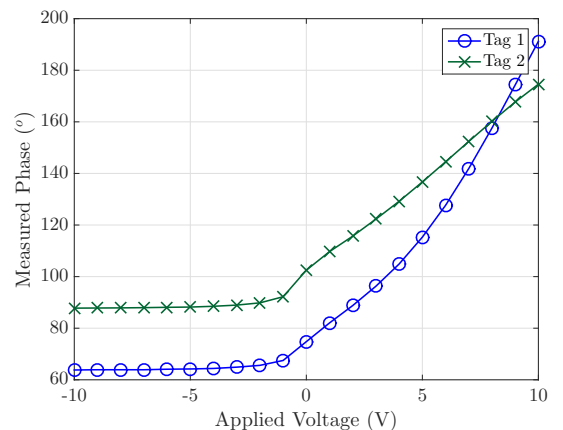


Fig. 4: Phase of reflection coefficient Γ_m acquired using a VNA. The two tags use different values for the coupling feed through capacitor.

the ramp was set to 100 ms (10 Hz). The value was chosen experimentally after observing the performance of the system. The chosen value would vary between communication systems/protocols (different from RFID Gen2) and propagation environments.

V. EVALUATION

A. Simulation Results

Verification of the proposed idea and its analysis in Sec. III was first conducted through simulations. Each slot affected

⁵It is evident that the selection of loads is critical to the performance of the assistive tag(s).

Phase Distribution	Fig. 5	Fig. 6 Setup (1)	Fig. 6 Setup (2)
Direct Channel (ϕ_0)	$\mathcal{U}[0, 2\pi)$	$\mathcal{U}[0, \pi)$	$\mathcal{U}[0, \pi/2)$
Tag #1 (ϕ_1, ϕ'_1)	$\mathcal{U}[0, 2\pi)$	$\mathcal{U}[0, \pi/4), \mathcal{U}[\pi, 1.9\pi)$	$\mathcal{U}[0, \pi/4), \mathcal{U}[\pi, 1.9\pi)$
Tag #2 (ϕ_2, ϕ'_2)	$\mathcal{U}[0, 2\pi)$	-	-
Rest Tags (ϕ_m, ϕ'_m)	$\mathcal{U}[0, 2\pi)$	-	-

TABLE I: Simulation parameters. $\mathcal{U}[a, b]$ denotes the uniform distribution of support $[a, b]$.

$N_G = 20$ transmission phases/interrogations and the simulations were performed using $N_S = 10$ slots. As described in Sec. IV, a ramp was used to control the varactor at the assistive tag. Thus, in the simulation setup, based on the assistive tags' phases (tag #1: 63° to 180° , tag #2: 80° to 150°), a staircase-approximated ramp consisting of N_S stairs/slots was used. Analysis results were calculated using Eq. (17) and the integral of Eq. (18) was evaluated using trapezoidal approximation. Exact and lower bound alignment probability was also estimated through Monte Carlo simulation. Channel phases were modeled as per Table I and the related PDF/CDFs were calculated according to [30].

Fig. 5-left offers the exact probability of alignment (through simulations), the lower bound of Eq. (15) (through simulations) and the analytical expression for the lower bound (Eq. (18)), for sector angle $\epsilon = 2.8^\circ$. The cases of one or two assistive tags are examined. It can be seen that there is good match between analysis and simulation results. Intuitively, the more assistive tags are utilized, the lower the probability of alignment will be. That is due to the fact that the more vectors are involved, the "harder" for all of them to align within a sector of angle ϵ . This intuition is supported by the offered results. The average number of alignment events per N_S slots is also depicted in the figure. It is noted that multiple (N_G) interrogations are "included" in each slot. Thus, λ_a represents the worst-case scenario for the number of successful interrogations due to alignment.

Fig. 5-right offers the probability of alignment when the sector size ϵ is varied, for a given slot. Intuitively, a larger sector size ϵ offers a larger area where channel vectors can coincide, increasing the number of alignment events. Thus, a larger sector size increases the alignment probability. However, increasing the sector size reduces the achievable beamforming gain, as will be subsequently shown (Sec. V-C4, Eq. (24)).

The probability of alignment is given for the cases of 2 to 5 tags. It can be seen that the probability decreases by (approximately) an order of magnitude for each additional assistive tag. In Fig. 5, the phases introduced by each tag were randomly selected (but held constant for the simulations); channel modelling is given in Table I. As more assistive tags are introduced in the system, more terms appear in the product of Eq. (17). This fact can explain the increase in "nonlinearity" for the lower values of ϵ . It has to be emphasized that the exact behaviour of the probability of alignment is modelling-dependent.

The results in Fig. 5-left show that the probability of alignment is steady for the whole duration of N_S slots. That is because of the symmetry of the involved distributions and the fact that channel phases can take values across the full $[0, 2\pi)$

range; all phases follow a uniform distribution with the same parameters (Table I).

On the contrary, results in Fig. 6-right demonstrate the effect of using different parameters in the involved distributions. The transient response of the system in that figure is justified by the fact that during the first slots, the rotating vector (due to $\Theta_m[k]$) of the assistive tag in conjunction with the range of the channel phases, results to a setup in the complex plane where it is impossible for an alignment to happen. An example of such setup is depicted in Fig. 6-left, for one assistive tag, at slot $k = 1$; the range of possible values for the involved phases of the two vectors, corresponding to the two channels cannot coincide within the sector, for the specific slot. The above conclusion is further supported by the fact that in Setup (2), where the phase of the direct channel is limited to $[0, \pi/2)$ (in contrast to $[0, \pi)$ of Setup (1)), the transient in the alignment probability occupies a greater number of slots.

B. Experimental Results-Interrogation Performance

Experiments were performed using a Thing Magic Sargas RFID reader, connected to an MTI MT-242032 7 dBi (nominal gain) antenna, via a 0.4 dB loss coaxial cable. Throughout the experiments, the reader was configured for RFID tag communication in dynamic Q mode, with backscatter link frequency (BLF) of 250 kHz and Miller-8 line coding. The distributed beamforming gain, due to the operation of backscattering tag(s) assisting interrogation of RFIDs, was showcased with two experiments, described below.

1) *RFID Tag Interrogation-No Mobility*: The reader was configured to output a signal at 20 dBm. A group of 5 ALN-9740 (Higgs-4) RFIDs was used. The RFIDs were randomly scattered in a radius of ≈ 0.2 m (see inlay of Fig. 8-right). Experiments were carried out at 3 random locations, 1.80 m, 2.16 m and 1.70 m away from the reader. At each of those locations, the assistive tag was placed at 4 random spots in the vicinity of the RFIDs.

The interrogation results as reported by the reader (averaged over 3, one minute-long, runs), for the first location (1.80 m away from the reader), are offered in Fig. 7. For each of the 4 (randomly selected) assistive tag spots, 3 cases were examined. The number of successful interrogations (reads) for each RFID in the absence of the assistive tag, is offered in the left-most bar of each spot. The middle bar offers the number of reads for the case of the assistive tag being present but not operating, while the right-most bar represents the case of the assistive tag being active. Looking into spot 3 of Fig. 7, the contribution of the assistive tag to the interrogation performance is evident: while in the absence of the tag only 3 RFIDs could be interrogated (A,C and E), with the assistive tag operating **all** RFIDs (A-E) were interrogated hundreds of times/minute (≈ 600 reads/min for each RFID).

Examining the results for the remaining spots, some interesting observations are made. First, even when the assistive tag is inactive (middle bar), interrogation gains can be offered (see spot 4, Fig. 7). This is expected, as the presence of the assistive tag alters the propagation environment and RFIDs at certain locations can enjoy gains. When inactive, the assistive's

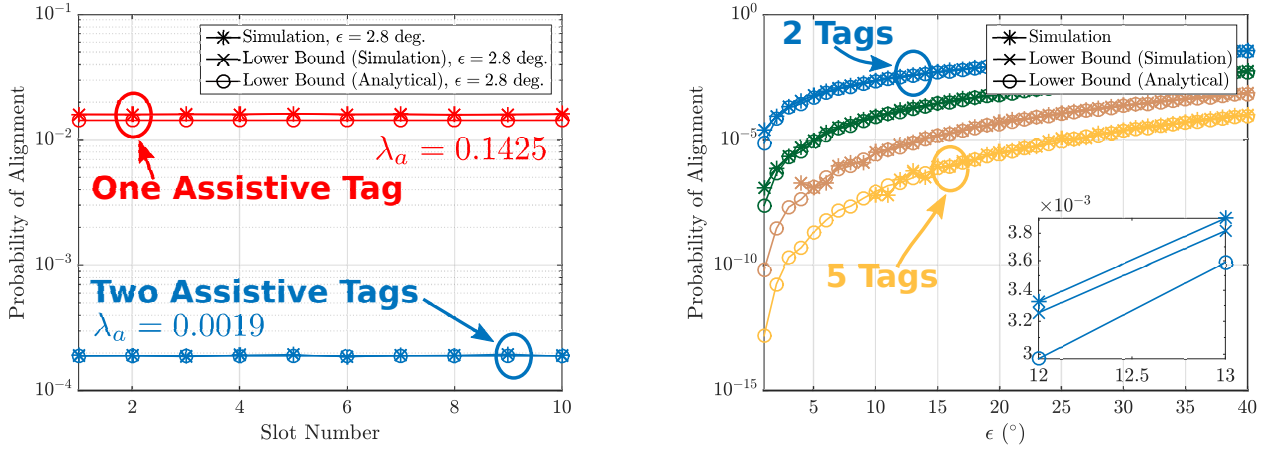


Fig. 5: (Left) Simulated probability of alignment, the lower bound of Eq. (15) and the analytical expression for the lower bound (Eq. (18)), for $\epsilon = 2.8^\circ$. The cases of both a single and two assistive tags are examined. (Right) Probability of alignment as a function of sector size ϵ , for 2 to 5 assistive tags.

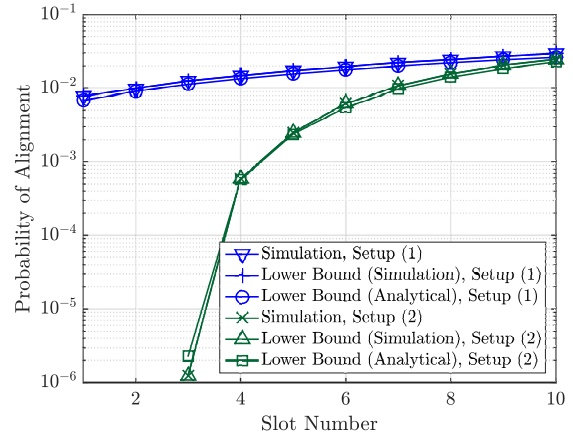
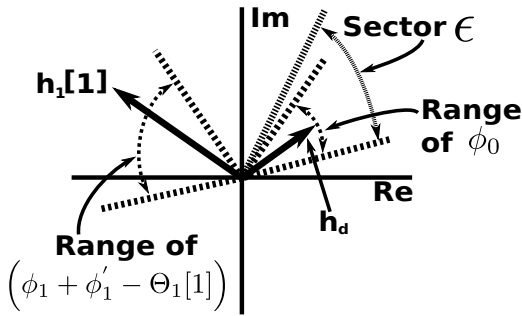


Fig. 6: (Left) In certain slots, the range of relevant phases may deem alignment impossible (within an alignment sector ϵ). (Right) Behavior of the system when phases introduced by the involved wireless channels have a limited range.

antenna is isolated from the diode using a transistor (see Sec. IV). The isolation leads to the assistive introducing a phase to the channel which is different from the phases introduced during normal operation. The “inactive” phase may offer destructive additions at some (RFID) locations (e.g., spot 1, RFID A) and constructive at others (spot 1, RFID D). In order to maximize the number of successfully interrogated RFIDs, the operation of the assistive can be duty-cycled; while the voltage applied to the diode is swept across its full range, a square wave can be applied to the assistive tag’s transistor for periodic activation/deactivation. Operating the assistive in such a manner would result, in spot 4 for example, successful interrogations of all RFIDs.

Results from the experiments in the second location, 2.16 m away from the reader, are given in Fig. 8-left (the setup is shown in Fig. 8-right). Considering spots 1, 3 & 4, it can be clearly seen that the assistive tag, despite the apparent strong multipath conditions in the location, helps the interrogation of a number of RFIDs. The effectiveness of the assistive tag can be improved by further improvement of its circuit, so as to

offer a wider range of capacitance (and by extension phase) values. It is noted that after the experiments at the second location were carried out, the group of RFIDs was moved at a direct LOS spot, 2.16 m in front of the reader’s antenna. At that direct LOS location, only RFIDs A, B & E were successfully interrogated. In the third location, 1.70 m away from the reader, no successful interrogations were reported, either with or without the assistive tag.

2) *RFID Tag Interrogation-Mobility*: Multiple RFID tags where deployed in an area 3 m away from the reader, with the latter configured to output a signal at 24 dBm (Fig. 9). Both Higgs-4 and Higgs-2 RFIDs were used; tag A was an older Higgs-2 RFID while B, C & D were Higgs-4. Both A and B were placed in a spot offering a direct LOS path to the reader, while RFIDs C and D were placed off the maximum gain direction of the reader antenna.

Three cases were evaluated; in the first case, interrogations were performed without any movement or any assistive tag operating; in the second case, a person was walking in the same pattern around the tags (Fig. 9); in the third, the same

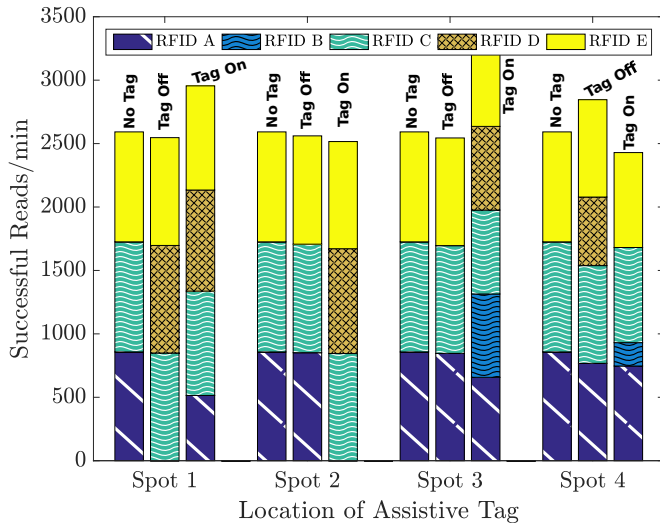


Fig. 7: Experimental results of the interrogation performance for 5 RFIDs using one assistive tag, at a distance of 1.80 m away from the reader. Both the RFIDs' and the assistive tag locations were randomly chosen. 3 cases per spot are examined: no assistive tag, assistive tag present but not operating, assistive tag active.

walking pattern was performed but with the person holding an assistive tag in operation. Results are offered in Fig. 10. It is shown that while mobility in the environment helps the interrogation of RFIDs located in spots where propagation conditions are not favorable, assistive tags offer an additional (to mobility) gain. For example, while tag C was not "seen" by the reader in a static environment, mobility offered (on average) 83.6 reads/minute, while mobility with the assistive tag offered 131.7 reads/minute. It was also observed that the read rate was increased at the time instants when the assistive tag was passed at certain angles in front of tags C, D, implying that mobility could be deemed unnecessary if the assistive was placed in the correct spot.

While the phase range of the assistive tag is fixed by design (depends on the circuit), moving the tag in space allows for the channel phases to vary across a wider range. Thus, the chances of the assistive tag to introduce a phase aligned with the rest of the multipath components are increased. The decrease in the read numbers of tags A, B (compared to the immobile case) is likely due to blocking of the direct paths during walking in front of these RFID tags.

C. Channel Measurement & Simulation Results

The effects of the assistive tags' operation in the wireless channel, were assessed using a two-port VNA. The VNA was configured in CW mode at a frequency of 867.5 MHz with an output power of -5 dBm. The transmitting antenna (MTI, see Sec. V-B) was connected to port 1 of the analyser and the receiving (a 1.8 dB bow-tie dipole) to port 2. The analyser was configured to report the value of the ratio $\frac{b_2}{a_1}$, which, assuming perfect termination of the receiving antenna (matched to port 2), is the transfer function between the

transmitting and receiving antennas (i.e., the wireless channel). The setup is shown in Fig. 11.

1) *Interrogation rate-Fixed assistive state*: An Impinj speedway R420 RFID reader was used, with output power of 20 dBm. An RFID (ALN-9540, Higgs-2) was placed 1.68 m away from the transmitting antenna and the performance of the reader for a fixed amount of time (10 s) was evaluated at 1000 interrogations (i.e., ~ 100 interrogations/sec). While maintaining the same distance, the RFID was moved to a second location where the reader could not interrogate it. The assistive tag was then placed at a distance of 23 cm from the RFID. While varying the voltage of the assistive's diode, the number of successful interrogations was recorded. The results are shown in Fig. 12.

Having recorded the number of successful interrogations, the RFID was replaced with the Rx antenna of the VNA (reader's antenna was connected to port 1 of the VNA). The Tx to Rx pathloss without the assistive tag being present was measured at -33.2 dB, while with the assistive tag being present but not operating, at -34.1 dB.⁶ The pathloss for two states of the diode is depicted in Fig. 12. It can be seen that when the assistive's diode is biased at 9 V, a gain of 1.6 dB is offered, while at 0 V, the measured gain is 0.9 dB. As it can be seen, a gain of 1.6 dB is enough for the tag to operate and be successfully interrogated multiple times.

2) *Interrogation rate-switching between two states*: Based on the results of Fig. 12, experiments utilizing switching between loads were carried out. In the first experiment the diode's voltage was switched between 0V and 9V and in the second between -5 V and 5V, at a rate of 1Hz. The interrogation rate was recorded and then the VNA was used to probe the channel. The results are shown in Fig. 13.

The interrogation rates depicted in Fig. 13-right, come in agreement with the results of Fig. 12: for the 0/9V switching, the assistive tag is 50% of the time in state 0V offering (on average) 2.6% successful interrogations and 50% in state 9V offering 98.9% successful interrogations. Thus, theoretically, an overall rate of 50.7% successful interrogations will be offered which is very close to the rate of 49.8% reported by the switching experiment (shown in Fig. 13-right). The same holds for the case of -5 /5V switching. The VNA traces of the channel pathloss and phase, for the switching experiments, are also shown in Fig. 13-left and center, respectively. It can be seen that, a maximum gain of 1.6 dB can be achieved while switching between appropriate loads.

3) *Achievable gain (experimental) vs RFID-Assistive tag distance*: To demonstrate the variability of the offered gain among different locations (in the same propagation environment), experiments were carried out using the aforementioned VNA-based method (Fig. 11). It has to be noted that the experiments of this section were carried out in a different location from the experiments of the previous sections. The assistive tag, driven by a ramp waveform (Fig. 3), was placed at a distance from the Rx antenna, which was varied from

⁶Measurements averaged over a 5 s time window in a environment with minimal-to-none mobility. The assistive tag being present but not operating (Tag Off) corresponds to a state where the transistor is off, i.e., the diode is disconnected from the antenna.

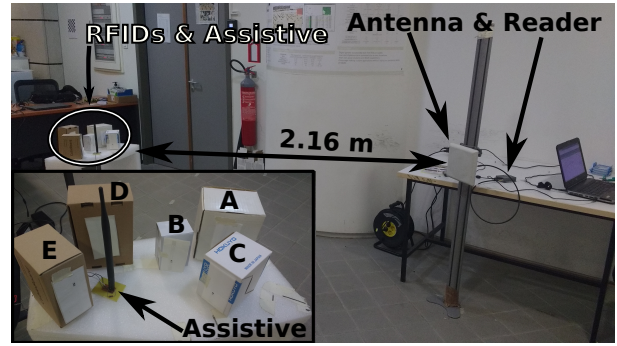
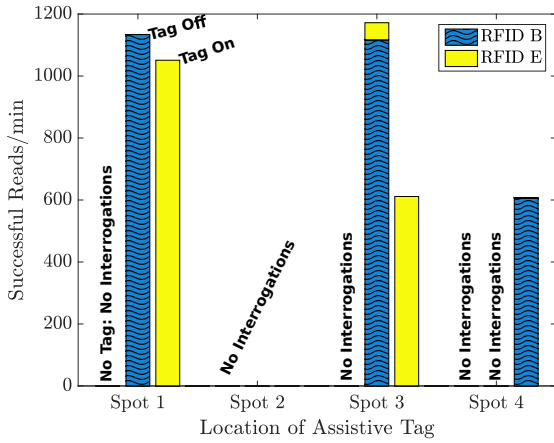


Fig. 8: (Left) Experimental results for the interrogation performance using a single assistive tag and 5 RFIDs. (Right) Setup utilized for the aforementioned measurements, 2.16 m away from the reader.

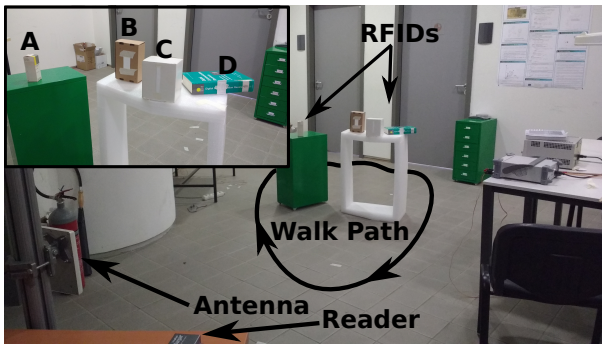


Fig. 9: Interrogation of multiple “ghost” RFIDs by altering the propagation conditions, either with mobility or with mobility in conjunction with an assistive tag. The environment of the experiment was arranged differently, compared to that of Sec. V-B1.

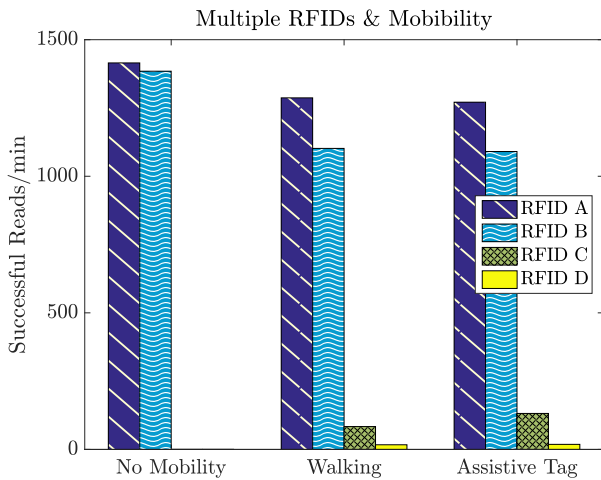


Fig. 10: Results of interrogating 4 different RFID tags under different conditions. Assistive tag was used while walking (holding it) around the tags. Results are averaged from ten 1-minute interrogation runs for each scenario.

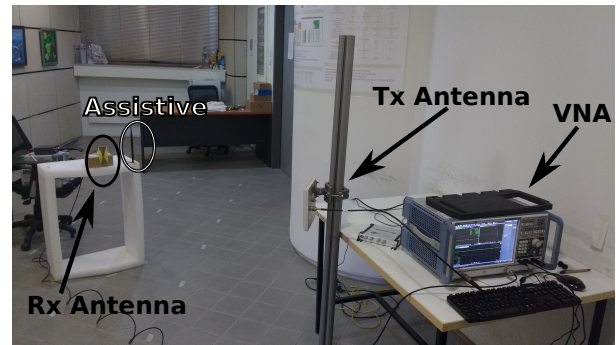


Fig. 11: Experimental setup for the assessment of assistive tags’ contribution to the wireless channel. The VNA was configured so as to measure the transfer function (channel) between the Tx antenna (port 1) and Rx antenna (port 2).

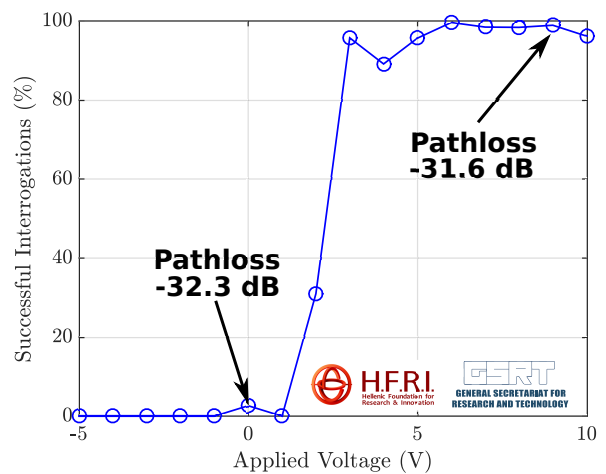


Fig. 12: Percentage of successful interrogations (out of 1000) as a function of the reverse bias voltage applied to the assistive’s diode. The interrogation rate was a result of averaging the number of successful interrogations over multiple runs (each run consisted of 1000 interrogations).

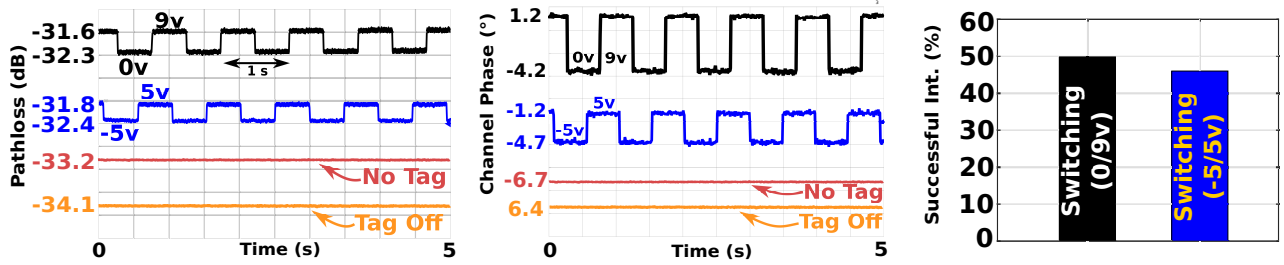


Fig. 13: Channel pathloss (Left), phase (Middle) and successful interrogation rate (Right), for the case of switching the termination of the assistive's antenna between two loads. A maximum gain of 1.6 dB is achieved for a reverse bias voltage of 9V. The “No Tag” label corresponds to the absence of the assistive tag.

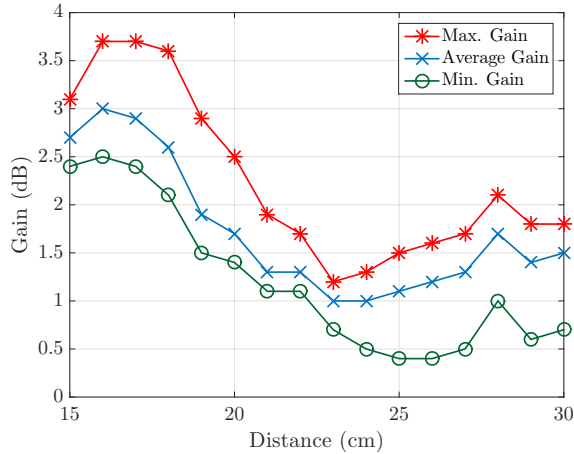


Fig. 14: Variation of the achievable gain as a function of the Rx-to-assistive tag distance.

15 to 30 cm. The resulting gain is offered in Fig. 14. As it is expected, gain has a decreasing oscillation as the distance increases. Therefore, the assistive tag should not be placed relatively far from the Rx antenna. Experimental results in Fig. 14 show gain values in the range of 0.4 – 3.7 dB.

4) *Achievable Gain-One & Two Assistive tags:* To assess the gain offered by a number of assistive tags, experiments and simulations were carried out and compared with the theoretical model of Eq. (24). Specifically, the cases of one and two tags were examined. The antenna gains used in the model were $G_R = 5$ dB,⁷ $G_A = 3$ dB, $G_G = 1.8$ dB. The distances utilized in the pathloss model (and in the experimental setup) were $d_0 = 1.68$ m, $d_{1,RA} = 1.65$ m, $d_{2,RA} = 1.77$ m, $d_{1,AG} = 0.23$ m, $d_{2,AG} = 0.16$ m. It has to be noted that the locations of the RFID and of the two assistive tags were arbitrarily chosen. Given a range of phases offered by the assistive tag, different setups will exhibit different gains.

Assuming an alignment event at t^* , variables $\tilde{\gamma}_m$ are defined as in Eq. (6), with $\tilde{\gamma}_0 = \sqrt{L_0}a_0$ and $\tilde{s}_m = s_m\gamma_m(t^*) = \sqrt{0.6}$ (scattering efficiency). Fading coefficients are assumed to

follow a Rician distribution:

$$a_j^{(m)} = |h_j^{(m)}|, \quad h_j^{(m)} \sim \mathcal{CN}\left(\sqrt{\frac{k_j^{(m)}}{k_j^{(m)} + 1}}\sigma_h, \frac{\sigma_h^2}{k_j^{(m)} + 1}\right), \quad (25)$$

where $m \in \{\emptyset, 1, 2\}$, $j \in \{0, RA, AG\}$, $\sigma_h^2 = 1$ and $\mathcal{CN}(\mu, \nu)$ denotes the proper complex Gaussian distribution of mean μ and variance ν . The Rician factor $k_j^{(m)}$ is set to $k_j^{(m)} = 20$. It can be shown that $\mathbb{E}\left[\left(a_j^{(m)}\right)^2\right] = \sigma_h^2$ [24]. Given the definition in Eq. (25), the expected value $\mathbb{E}\left[a_j^{(m)}\right]$ is given by [31]:

$$\mu_j^{(m)} = \mathbb{E}\left[a_j^{(m)}\right] = \sqrt{\frac{\pi\sigma_h^2}{4(k_j^{(m)} + 1)}} {}_1F_1(-1/2; 1; -k_j^{(m)}), \quad (26)$$

where ${}_1F_1(a; b; c)$ is the confluent hypergeometric function of the first kind [32]. Eq. (24) can then be used to analytically offer the average gain.

The channel h^* , as per Eq. (21), was simulated. Alignment within a sector ϵ was achieved by modelling the associated phases as $\tilde{\phi}_m \sim \mathcal{N}(0, \epsilon^2/2)$; $\mathcal{N}(\mu, \nu)$ denotes the Gaussian distribution of mean μ and variance ν . The simulated impinged power was defined as the numerical average of $P_{tx}|h^*|^2$, across 10^5 channel realizations. The gain was then calculated as the ratio of the aforementioned average power to the numerical average of $P_{tx}|h_d|^2$.

To experimentally measure the offered gain, the setup described earlier (utilising the VNA) was used. The pathloss without any assistive tag present was measured at -33 dB. Measurements were conducted utilising only one tag at a time. The maximum gain offered by tag #1 was 1.8 dB, while tag #2 offered 1.5 dB (operating as in Fig. 3). Then, both tags were placed near the Rx antenna and unsynchronized ramp waveforms of the same parameters (see Sec. IV) were used to drive them (the ramp's frequency was set to 1 Hz for the VNA measurements). The maximum gain was 2.9 dB.

Fig. 15 offers the average gains when using 1 and 2 assistive tags, as a function of sector size. Additionally, the experimental gains are depicted. It can be seen that the approximate average gain offered by Eq. (24) matches to the simulation results. The behaviour (w.r.t. sector size) of the analytical expression (and the simulation results) will depend on the modelling of the phases ($\tilde{\phi}_m$). Furthermore, it is evident that

⁷The reader's antenna has a nominal gain (at the direction of its main lobe) of 7 dB. The Rx antenna (and the RFID) is placed at a direction lying outside its main lobe, thus the gain is reduced.

the predictions from the model and the simulations, are a close match for the measurement/experimental results, with a maximum error of ≈ 0.4 dB.

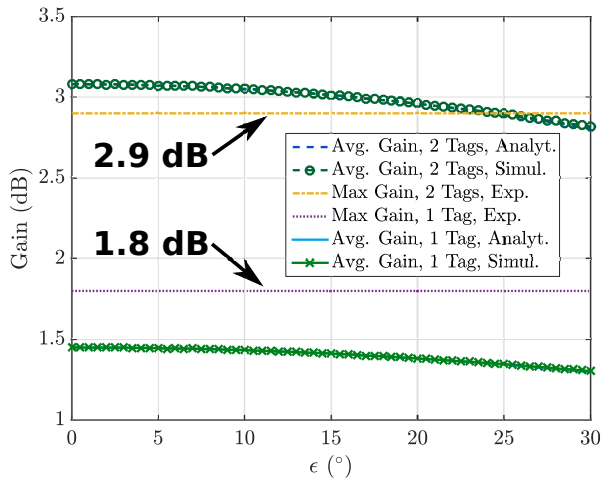


Fig. 15: Analytical and simulated average power gain for the cases of 1 and 2 assistive tag(s) as a function of sector size (ϵ). Experimental power gain for the two cases is also given as measured by the VNA. The lines representing the experimentally measured gain exist only for comparison purposes.

VI. CONCLUSION

This work offered a simple, *zero-feedback*, beamforming technique that aids the reception of signals, subject to multipath conditions. Exploiting backscatter radio principles, assistive backscattering tags were implemented, capable of varying the phase of an impinged signal and thus, altering the propagation conditions. It was experimentally shown that the proposed beamforming tags can offer power gains in the range of 0.4–3.7 dB. In contrast to prior art, the proposed technique did not utilize any channel-related information (zero-feedback) or elaborate control algorithms. Although tested on the RFID Gen2, the *simple*, zero-feedback nature of the proposed assistive tag(s), could assist different radio standards.

REFERENCES

- [1] N. D. Sidiropoulos, T. N. Davidson, and Z.-Q. Luo, "Transmit beamforming for physical-layer multicasting," *IEEE Trans. Signal Processing*, vol. 54, no. 6, pp. 2239–2251, Jun. 2006.
- [2] T. Ohira and K. Iigusa, "Electronically steerable parasitic array radiator antenna," *Electronics and Communications in Japan (Part II: Electronics)*, vol. 87, no. 10, pp. 25–45, 2004.
- [3] C. Sun, A. Hirata, T. Ohira, and N. C. Karmakar, "Fast beamforming of electronically steerable parasitic array radiator antennas: theory and experiment," *IEEE Trans. Antennas Propagat.*, vol. 52, no. 7, pp. 1819–1832, Jul. 2004.
- [4] A. Kalis, A. G. Kanatas, and C. B. Papadias, "A novel approach to mimo transmission using a single rf front end," *IEEE J. Select. Areas Commun.*, vol. 26, no. 6, pp. 972–980, Aug. 2008.
- [5] A. Kalis, A. Kanatas, and C. Papadias, *Parasitic Antenna Arrays for Wireless MIMO Systems*. Springer, 2013.
- [6] C. Plapous, J. Cheng, E. Taillefer, A. Hirata, and T. Ohira, "Reactance domain music algorithm for electronically steerable parasitic array radiator," *IEEE Trans. Antennas Propagat.*, vol. 52, no. 12, pp. 3257–3264, Dec. 2004.
- [7] R. Mudumbai, D. R. Brown, U. Madhow, and H. V. Poor, "Distributed transmit beamforming: challenges and recent progress," *IEEE Commun. Mag.*, vol. 47, no. 2, pp. 102–110, Feb. 2009.

- [8] A. Bletsas, A. Lippman, and J. N. Sahalos, "Simple, zero-feedback, distributed beamforming with unsynchronized carriers," *IEEE J. Select. Areas Commun.*, vol. 28, no. 7, pp. 1046–1054, Sep. 2010.
- [9] D. M. Dobkin, T. Freed, C. Gerdorn, C. Flores, E. Futak, and C. Suttner, "Cooperative tag communications," in *Proc. IEEE RFID Techn. and Applications (RFID-TA)*, Tokyo, Japan, Sep. 2015, pp. 27–32.
- [10] N. Kaina, M. Dupre, G. Lerosey, and M. Fink, "Shaping complex microwave fields in reverberating media with binary tunable metasurfaces," *Scientific Reports*, vol. 4, p. 6693, Oct. 2014.
- [11] M. Dupré, P. del Hougne, M. Fink, F. Lemoult, and G. Lerosey, "Wave-field shaping in cavities: Waves trapped in a box with controllable boundaries," *Phys. Rev. Lett.*, vol. 115, p. 017701, Jul. 2015.
- [12] M. Di Renzo *et al.*, "Smart radio environments empowered by reconfigurable AI meta-surfaces: an idea whose time has come," *EURASIP Journal on Wireless Communications and Networking*, vol. 2019, no. 1, p. 129, May 2019.
- [13] E. Basar, M. Di Renzo, J. de Rosny, M. Debbah, M.-S. Alouini, and R. Zhang, "Wireless Communications Through Reconfigurable Intelligent Surfaces," Jun. 2019. [Online]. Available: <https://arxiv.org/abs/1906.09490>
- [14] X. Tan, Z. Sun, J. M. Jornet, and D. Pados, "Increasing indoor spectrum sharing capacity using smart reflect-array," in *Proc. IEEE Int. Conf. Communications*, May 2016, pp. 1–6.
- [15] C. Liaskos, S. Nie, A. Tsioliaridou, A. Pitsillides, S. Ioannidis, and I. Akyildiz, "A new wireless communication paradigm through software-controlled metasurfaces," *IEEE Commun. Mag.*, vol. 56, no. 9, pp. 162–169, Sep. 2018.
- [16] S. Han and K. G. Shin, "Enhancing wireless performance using reflectors," in *Proc. IEEE INFOCOM*, May 2017, pp. 1–9.
- [17] Z. Li, Y. Xie, L. Shanguan, R. I. Zelaya, J. Gummeson, W. Hu, and K. Jamieson, "Towards programming the radio environment with large arrays of inexpensive antennas," in *16th USENIX Symposium on Networked Systems Design and Implementation (NSDI 19)*, Boston, MA, Feb. 2019, pp. 285–300.
- [18] V. Arun and H. Balakrishnan, "RFocus: Practical beamforming for small devices," 2019. [Online]. Available: <http://arxiv.org/abs/1905.05130>
- [19] Greenerwave, last Visited 27/9/19. [Online]. Available: <http://greenerwave.com/>
- [20] G. Lerosey *et al.*, "Waveforming device and wave receiver," May 2019, Patent FR3066665B1. [Online]. Available: <https://patents.google.com/patent/FR3066665B1>
- [21] P. del Hougne, M. Fink, and G. Lerosey, "Shaping microwave fields using nonlinear unsolicited feedback: Application to enhance energy harvesting," *Phys. Rev. Applied*, vol. 8, p. 061001, Dec. 2017.
- [22] J. D. Griffin and G. D. Durgin, "Multipath fading measurements at 5.8 GHz for backscatter tags with multiple antennas," *IEEE Trans. Antennas Propagat.*, vol. 58, no. 11, pp. 3693–3700, Aug. 2010.
- [23] G. Vannucci, A. Bletsas, and D. Leigh, "A software-defined radio system for backscatter sensor networks," *IEEE Trans. Wireless Commun.*, vol. 7, no. 6, pp. 2170–2179, Jun. 2008.
- [24] A. Goldsmith, *Wireless Communications*. New York, NY, USA: Cambridge University Press, 2005.
- [25] A. Bletsas, A. G. Dimitriou, and J. N. Sahalos, "Improving backscatter radio tag efficiency," *IEEE Trans. Microwave Theory Tech.*, vol. 58, no. 6, pp. 1502–1509, Jun. 2010.
- [26] J. D. Griffin and G. D. Durgin, "Complete link budgets for backscatter-radio and RFID systems," *IEEE Antennas Propagat. Mag.*, vol. 51, no. 2, pp. 11–25, Apr. 2009.
- [27] A. Pappoulis and S. U. Pillai, *Probability, Random Variables and Stochastic Processes*, 4th ed. New York, NY: McGraw-Hill, 2002.
- [28] B. B. van der Genugten, "The distribution of random variables reduced modulo a," *Statistica Neerlandica*, vol. 26, no. 1, pp. 1–13, 1972.
- [29] A. G. Dimitriou, J. Kimionis, A. Bletsas, and J. N. Sahalos, "A fading-resistant method for RFID-antenna structural mode measurement," in *2012 IEEE International Conference on RFID-Technologies and Applications (RFID-TA)*, Nice, France, Nov. 2012, pp. 443–448.
- [30] F. Killmann and E. von Collani, "A note on the convolution of the uniform and related distributions and their use in quality control," *Economic Quality Control - Econ Qual Contr*, vol. 16, pp. 17–41, Jan. 2001.
- [31] C. G. Koay and P. J. Basser, "Analytically exact correction scheme for signal extraction from noisy magnitude MR signals," *Journal of Magnetic Resonance*, vol. 2, pp. 317–322, 2006.
- [32] M. Abramowitz and I. A. Stegun, Eds., *Handbook of Mathematical Functions with Formulas, Graphs, and Mathematical Tables*. U.S. Government Printing Office, Washington, D.C., 1964.